Available online at www.sciencedirect.com

ScienceDirect

Materials Today: Proceedings 5 (2018) 22630–22637

materialstoday: PROCEEDINGS

www.materialstoday.com/proceedings

ICASE_2017

Synthesis of BiOCl: Eu^{3+} Microarchitectures and Their WLED's, Fingerprint Detection and Anticounterfeiting Applications

Vinod Phadke[a*], S. Chandramma[b*], H. Nagabhushana[c], R.B.Basavaraj[c]

[a]*Department of Electronics, Kalpataru First Grade Science College, Tiptur-572 201, India*
[b]*Department of Electronics, Yuvaraja's College, Mysore, 570005*
[c]*Department of Physics, Tumkur University, Tumkur-572103*

Abstract

BiOCl: Eu^{3+}(1-9mol %) microarchitectures were synthesized by the solution combustion method by employing Barbituric acid as fuel. The crystal structure, morphologies and luminescence properties of Eu^{3+} doped BiOCl have been systematically investigated by powder X-ray diffraction (PXRD) and scanning electron microscopy (SEM) and spectroscopy respectively. The prime objective of the current effort was first to fabricate highly luminescent nanophosphor for revelation of latent fingerprints, lips prints including infiltrating and non-filtrating surfaces and also to develop luminescent ink for anticounterfeiting applications. Presently the fingerprints developed by using conventional powders have several disadvantages including low sensitivity, high background hindrance, complicated procedure and high toxicity. To encounter this challenge, we explored the optimized BiOCl:Eu^{3+}(3mol %) nanophosphor for detection of latent fingerprints and luminescent anti-counterfeiting ink. The morphology of the phosphor was tuned by adjusting the concentration of fuel. Photoluminescence studies of BiOCl:Eu^{3+}(1-9mol %) exhibited the peaks $^5D_0 \rightarrow {}^7F_J$ (J = 0, 1, 2, 3, 4) transitions. The CIE and CCT characteristics specify that the synthesized nanophosphor might be immensely show potential red factor for promising applications in WLED's. The BiOCl: Eu^{3+} (1-9 mol %) nanopowder also showed clear ridge patterns of level I and level II and further showed sharp image of label when observed in the UV light. The results indicated that the present phosphor could be used in both forensic as well as in anti counterfeiting applications.

Selection and/or Peer-review under responsibility ofInternational Conference on Advances in Science & Engineering ICASE - 2017.

*Keywords:*BiOCl, Barbituric acid, morphology, luminescence, Eu^{3+}, nanophosphor, photoluminescence

* Corresponding author. Tel.: 91-9964792012.
E-mail address: vinod.phadke@gmail.com

1. Introduction

In the recent scenario, rare earth (RE) doped phosphor converted white LED's creating much interest for researchers in the field of illumination because of their unique properties like lower energy consumption, highly reliable, high brightness, long lifetime and eco-friendly nature [1]. The luminescent materials having wide area application that includes anticounterfeiting inks, production of vitamin D, photochemical reactions, water purifiers, phototherapy and forensic science [2]. In view of these applications and advantages, the study of RE activated nanosized and nanostructured phosphors are making boom in the phosphor industries.

Due to improved quantum efficiency and ability to transfer efficient energy from host to RE ions, metal oxychloride makes fascinating choice. Among them, the host BiOCl is a semiconductor of family V-VI-VIII and creates interest due to its better photoluminescence properties, structural variability and ability [3]. Generally Bismuth is a p block metal with a d^{10} configuration. In a Bi^{3+} oxides, hybridized valence band (VB) is formed due to hybridization of Bi6s and O2p levels, which leads to photo generated holes [4]. Bismuth oxychloride (BiOCl) is a wide band gap semiconductor with a tetragonal matlockite (PbFCl-type) structure. Its unique crystal structure and more favourable substitution for rare earth ions will lead BiOCl as efficient host for photoluminescence. Therefore, BiOCl have a wide range of applications in battery material, photocatalysis, pigments, pharmaceutical and photo electrochemical devices [5, 6].

The nanomaterials(NPs) with different morphology, namely nano-belts, nano needles, nano-rods, nano bowls, nano nails, nano wires and nanoparticles were synthesized by different methods namely hydrothermal, solvothermal, chemical vapour deposition, ionothemal, high temperature method, sol–gel, direct precipitation, combustion synthesis etc.[7]. The majority of these synthesized routes involve sophisticated equipments, lethal procedures and meticulous experimental conditions. Conversely, synthesis of nanostructures (NS) is still a challenge to come across a simple fabrication process. At present, synthesis of NPs by avoiding use and generation of hazardous substances achieved by green synthesis strategy received great attention in research area due to nontoxic, environmentally kindly reactants/solvents and no release of hazardous byproducts. In Green synthesis method, naturally available supplies such as vitamins, sugars, plant extracts, biodegradable polymers and microorganisms were utilized and were used as capping agents. Materials from plant such as leaf, root, latex, seed, and stem emerge as a best reagents used for large-scale 'bio mediated synthesis' of NPs [8]. Moreover, green synthesis is a cost effective and eco-friendly approach.

In this paper BiOCl:Eu^{3+}(1-9mol%) microarchitectures were synthesized by the solution combustion method employing Barbituric acid as fuel. The crystal structure, morphology and luminescence properties of Eu^{3+} doped BiOCl have been systematically investigated by powder X-ray diffraction (PXRD), Scanning Electron Microscopy (SEM) and photo luminescence spectroscopy (PL) respectively.

2. Experimental

2.1. Synthesis

All the chemicals used are of analytical grade and were used without further purification. Bismuth nitrate pentahydrate [Bi(NO3)3.5H2O], ammonium chloride (NH4Cl) and concentrated nitric acid were taken in stoichiometric ratios and dissolved in a deionized water under vigorous stirring. The dopant Europium nitrate [Eu(NO3)3;(99.9 %] and the Barbituric acid used as a fuel, procured from Sigma Aldrich (C4H4N2O3) were dissolved in a previously prepared solution. Aqueous solution containing reactants is taken in a 300 ml cylindrical Pyrex petri dish. The dish is introduced into a muffle furnace maintained at a temperature of 400 ± 100C. The reaction mixture undergoes thermal dehydration and auto-ignites with liberation of gaseous products such as nitrogen and carbon. The flame propagates throughout the reaction mixture causing decomposition of the reactants, and subsequent formation of the desired product. The obtained product was calcined at 1000oC for 3h and used for characterization.

2.2. Characterization

The crystallinity and phase formation of the NP was carried out using a powder X-ray diffractometer (XRD, Shimadzu 7000). Cuk$_\alpha$ (1.541 Å) radiation with nickel filter was used to obtain diffraction data and a flatbed sample holder in transmission setup. The patterns were recorded with a 130° image plate detector at room temperature and ambient pressure. Scanning electron microscopy (SEM) measurements were performed on a Hitachi table top, Model TM 3000. The product was dispersed on a sticky carbon pad. To improve the image quality, a thin layer of Ag was deposited on the sample surface. By using Jobin Yvon Spectroflourimeter Fluorolog-3, the photoluminescence (PL) measurement were performed. These fluorescent NPs were successfully used for visualization of LFPs on porous and nonporous surfaces.

3. Result and discussions

3.1. Structural analysis

Figure 1(a) shows the Powder X-ray diffraction patterns of BiOCl:Eu^{3+} (1-9mol %) phosphors. The observed diffraction peaks corresponds to a matlockite-type tetragonal structure having the space group P4/nmm(No. 129) which is in agreement to the standard JCPDS card No. 85–0861 [9].

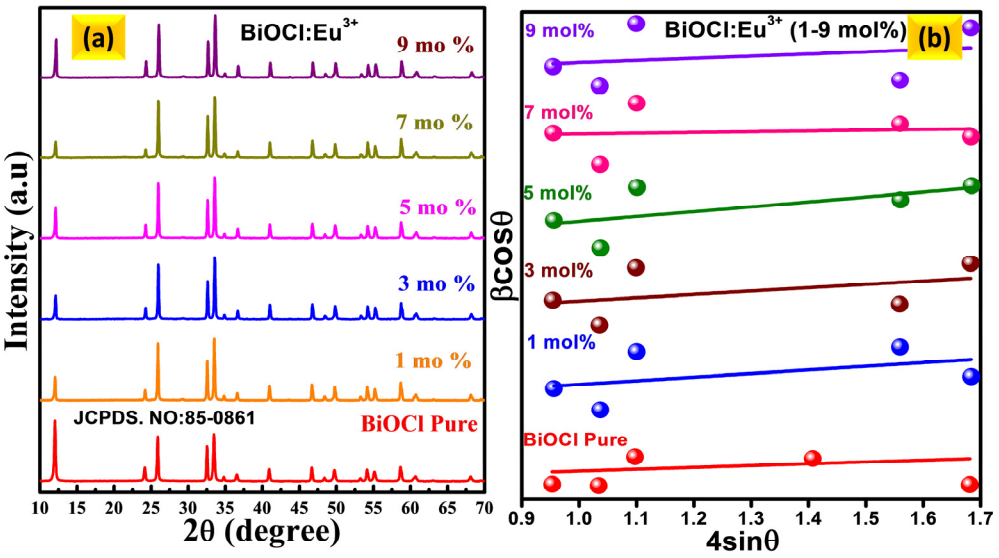

Fig.1 (a) PXRD patterns and (b) W-H plots of pure and Eu3+ (1-9 mol %) doped BiOCl nanostructures.

The average crystallite size (D) was calculated by using Scherrer's equation[10]. The obtained results are given in Table 1.

$$d = \frac{K\lambda}{\beta\cos\theta}$$

Where K;a constant, λ *; wavelength of X-rays, and* β *; FWHM.*

Fig 1(b) shows the W-H plots which were drawn with 4Sinθ along x-axis and βCosθ along y axis. Using this plot the average particle size was determined for different concentrations of Eu3+. The table (1) compares the estimated crystallite size values of BiOCl:Eu3+ (1-9mol%) NPs. using D-S and W-H methods respectively. The values of particle size were found to agree in both methods.

Table 1: Estimated crystallite size values of BiOCl:Eu^{3+} (1-9mol%) NPs.

Eu^{3+} conc. (mol %)	crystallite size (nm)	
	D-S approach	W-H plots
1	45	48
3	39	41
5	40	45
7	40	42
9	37	39

3.2. Morphological studies

Fig 2 shows the SEM micrographs of BiOCl: Eu^{3+} (3 mol %) prepared with different concentrations of Barbituric acid. It is observed that when the concentration of Barbituric acid was 1 wt% and 2wt%, a clear spherical shaped particles were formed (Fig.2a, b). However, with increase of concentration of Barbituric acid to 3 and 4% the particles start agglomeration and a tumour like morphology was observed (Fig.2c, d).

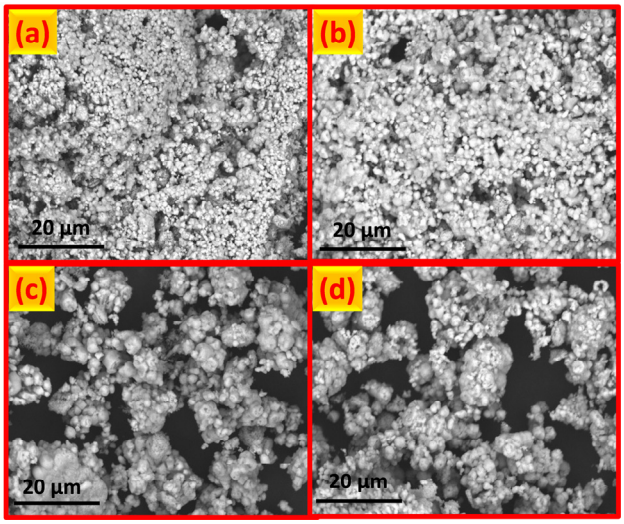

Fig.2 SEM micrographs of BiOCl:Eu^{3+}(3 mol%) prepared with different concentration of Barbituric acid, (a) 1 wt%, (b) 2 wt%, (c) 3 wt% and (d) 4 wt %.

3.3 Photoluminescence studies

The excitation spectrum of BiOCl:Eu^{3+} (3mol %) NP was recorded in the range 300-500 nm at an emission wavelength 610 nm is shown in inset Fig.3 (a). The spectrum shows sharp and intense peaks at ~ 361, 383, 394, 415, and 464 nm and were attributed to $^7F_0 \rightarrow {}^5D_4$, $^7F_0 \rightarrow {}^5L_7$, $^7F_0 \rightarrow {}^5L_6$, $^7F_0 \rightarrow {}^5D_3$, and $^7F_0 \rightarrow {}^5D_2$ transitions of Eu^{3+} ions in the host lattice site respectively [11]. Fig.3 (b) shows the emission spectra of BiOCl:Eu^{3+} (1-9mol %) nanophosphor under 397 nm excitation wavelength at room temperature (RT). The spectra exhibit peaks at ~ 536, 591, 610 and 651 nm and were attributed to $^5D_0 \rightarrow {}^7F_0$, $^5D_0 \rightarrow {}^7F_1$, $^5D_0 \rightarrow {}^7F_2$ and $^5D_0 \rightarrow {}^7F_3$ $4f^6$ configuration of Eu^{3+} ions, respectively [12]. The peak at 610 nm was electric–dipole transition $^5D_0 \rightarrow {}^7F_2$ which was much intense and hypersensitive in the host matrix. The weak emission peak at 591 nm was attributed to $^5D_0 \rightarrow {}^7F_1$ transition and ascribed to magnetic dipole transition which was insensitive to site symmetry. Asymmetry ratio (A_{21}) was used to determine the degree of distortion from the inversion symmetry of the local environment of the Eu^{3+} ions in the host was given by following equation [13]:

$$A_{21} = \frac{\int I_2\left({}^5D_0 \rightarrow {}^7F_2\right) d\lambda}{\int I_1\left({}^5D_0 \rightarrow {}^7F_1\right) d\lambda} \qquad \text{--------- (2)}$$

where I_1 and I_2; intensity at 610 nm and 591 nm respectively. In the present case, the value of A_{21} for BiOCl:Eu^{3+} (1-9mol %) NPs decreases with increase of Eu^{3+} concentration. The variation of A_{21} values with doping concentration can influence the luminescent property of a sample. It was evident that, intensity of emission peak (610 nm) was increased with increase of Eu^{3+} concentration up to 5 mol % and later diminishes. The distance between the two Eu^{3+} ions in BiOCl host was estimated by using critical energy transfer distance relation [14]:

$$R_c = 2\left(3V \big/ 4\pi N X_c\right)^{1/3} \qquad \text{---------- (3)}$$

Where V; unit cell volume, X_c; critical concentration of Eu^{3+} ions and N; number of crystallographic sites per unit cell. In the present case, calculated value of R_c was found to be ~ 14.21 Å. The value of R_c was greater than 5Å shows that electric multipolar interaction was the main reason of concentration quenching. The electric multipolar interaction involves dipole – dipole, dipole – quadrupole and quadrupole – quadrupole interactions. According to Dexter theory, the type electric multipolar interaction was estimated by using the following relation [15]:

$$\frac{I}{\chi} = K\left[1 + \beta(\chi)^{\frac{Q}{3}}\right]^{-1} \qquad \text{-------- (4)}$$

where χ ; concentration of Eu^{3+} ions, Q ; constant of electric multipolar interaction and K and β ; constants for the given host crystal under the same excitation condition. The estimated Q value was found to be 7.66 by linear fitting using Eq. (4) and was nearly equal to 8. This finding indicates that the charge transfer mechanism was due to dipole–quadrupole interaction for the concentration quenching in BiOCl:Eu^{3+} (1-9mol %) nanophosphor.

The CIE co-ordinates were estimated using PL emission spectra. The CIE chromaticity diagram corresponding to BiOCl:$Eu^{3+}$with different concentrations were shown in Fig.3 (c). It was noticed that the CIE co-ordinates for BiOCl:Eu^{3+} (x = 0.5386, y = 0.4684) for 3mol % was located in red region and nearly same as the National Television System Committee (NTSC) standard values of pure red color (0.67, 0.33) [16].The correlated color temperature (CCT) was one the important parameter to know the color appearance of the light emitted by a source, relating its color with respect to a reference light source when heated up to a specific temperature, in Kelvin (K). The CCT was calculated and showed in Fig.3 (d) by the method as reported earlier [17].

3.4 Forensic applications

The latent fingerprints (LFPs) are unique for each individual [18-19]. The prepared BiOCl: Eu^{3+} (3 mol %) nano powders were tested for forensic as well as anticounterfeiting applications. The optimized nanopowders were dusted

on various porous and nonporous substrate surfaces by using powder dusting method. Fig.4 depicts the latent fingerprints on aluminium foil, glass slide, steel plate and currency note respectively dusted with optimized nanopowder of BiOCl: Eu^{3+} (3 mol %). It can be observed from the figure that the clear ridge patterns including Level I (core) and Level II (bifurcation, ridge ending, island, eye etc.) were observed.

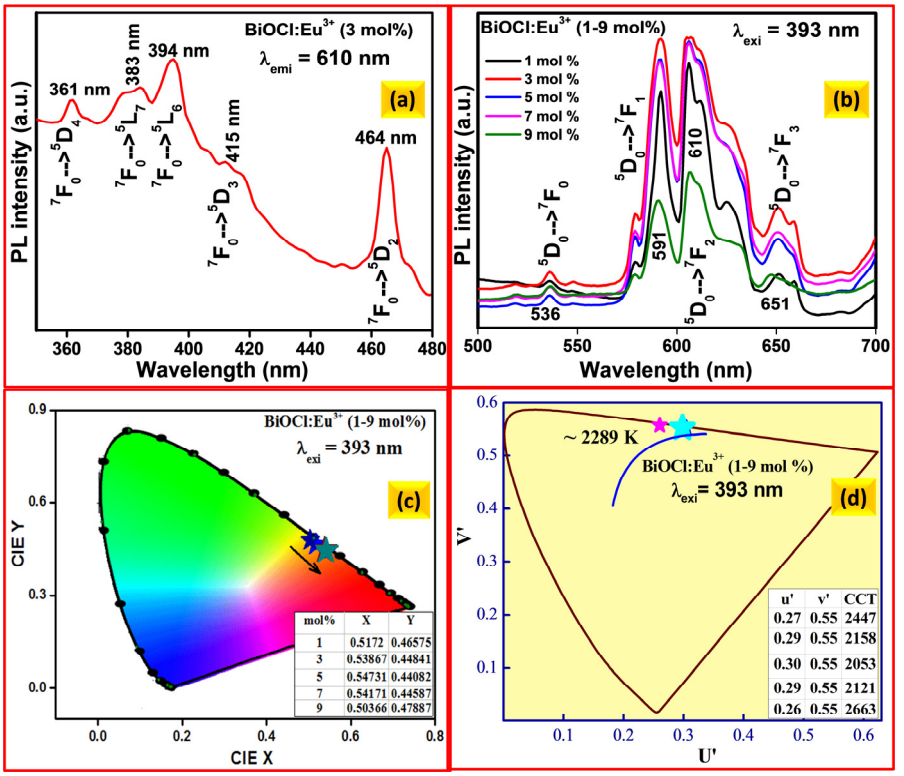

Fig. 3 (a) Excitation spectrum of BiOCl:Eu^{3+} (3mol %), (b) emission spectra of BiOCl:Eu^{3+} (1-9 mol %) nanophosphor under 393 nm excitation wavelength, (c) CIE and (d) CCT diagram of BiOCl:Eu^{3+} (1-9 mol %) nanophosphors.

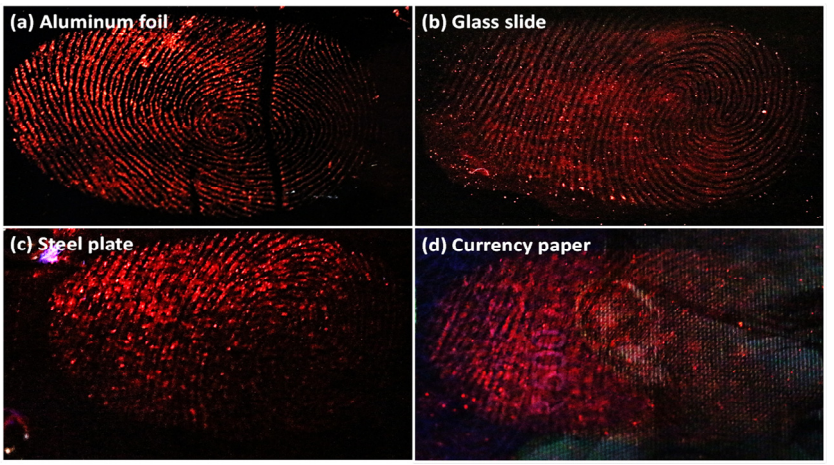

Fig.4 Latent fingerprint images of BiOCl:Eu^{3+} (3 mol %) on various material surfaces, (a) Aluminium foil (b) glass slide (c) steel plate and (d) currency paper.

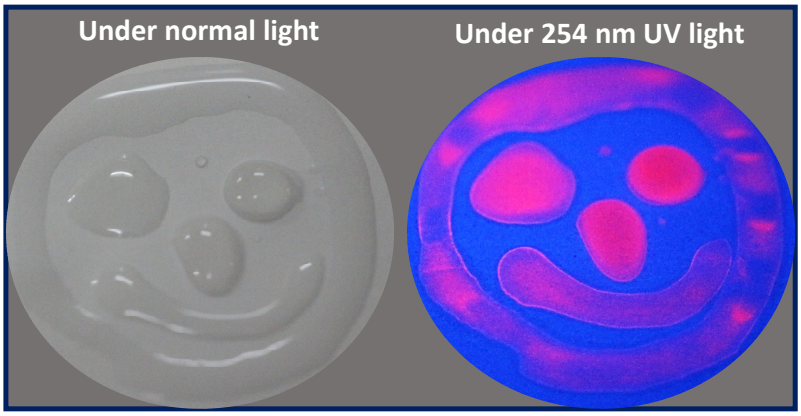

Fig.5 Anti-counterfeiting label painted with BiOCl: Eu^{3+} (3mol %) nanopowder ink under visible light and under 254 nm UV light excitation.

Fig.5 shows the digital photograph of anti-counterfeiting labels painted with BiOCl: Eu^{3+} (3 mol %) nanopowder ink under visible light and under 254 nm UV light excitation. The prepared NP was dispersed in water uniformly by means of ultrasonic irradiation and then used as a dip pen writing to draw different symbols. In the normal light it was fairly difficult to observe the clear image of the symbol. Under UV 254 nm light illumination, clear sharp image of the symbols were observed. The obtained results revealed that the prepared NP can also be used for anti-counterfeiting applications.

4. Conclusions

Eu^{3+} (1-9 mol %) doped BiOCl nanophosphors were synthesized by solution combustion method using Barbituric acid as fuel. The PXRD patterns shows that there was creation of micro-strain with the increase of Eu^{3+} dopant concentration in BiOCl nanophosphors resulting in broadening and shifting of peak position. The particle size estimated by Scherrer's method shows that the particle size decreases with increase of co-dopant concentration. This was in good agreement with the particles observed in SEM micrographs. The PL spectra taken for different excitation wavelengths showed splitting up of spectral lines due to local distortion induced by the co-dopant ion concentration. The PL spectra of 3 mol% Eu^{3+} ion doped BiOCl nanophosphors showed maximum intensity above which the intensity diminishes due to concentration quenching. The $^5D_0 \rightarrow {}^7F_2$ transition of BiOCl:Eu^{3+}showed larger optical gain to value, which was the required condition for lasing action and therefore it was highly useful for red laser application. The BiOCl:Eu^{3+} (1-9 mol %)nanopowder also showed clear ridge patterns of level I and level II and further showed sharp image of label when observed in the UV light. The results indicated that the present phosphor can be used in both forensic as well as in anti-security ink labels.

Acknowledgement

The author wishes to thank the Management of Kalpataru First Grade Science College, Tiptur, 572201 for their continued encouragement to carry out this research work.

References

[1] V.V. Rangari, S.J. Dhoble, Synthesis and photoluminescence studies of Ba(Gd,Ln)B9O6:Eu3+(Ln=La,Y) photophosphors for n-UV LED lighting and display devices. J.Rare Earths; 2015; 33:140-147.

[2] VijaySingh, S. Borkotoky, A. Murali, J.L. Rao, T.K. Gundu Rao, S.J. Dhoble. Spect. Electron paramagnetic resonance and photoluminescence investigation on ultraviolet-emitting Gadolinium-in-doped CaAl12O19 phosphors. chim. Acta Part A.2015;139:1-6.

[3] Chao Xue, Jiale Xia, Ting Wang, Shishun Zhao, Guidong Yang, Bolun Yang, Yanzhu Dai, Guang Yang. A facile and efficient solvothermal fabrication of three- dimensionally hierarchical BiOBr microspheres with exceptional photocatalytic activity. Mater. Lett. 2014;133:274-277.
[4] Lang Chen,Rui Huang, Miao Xiong,Qing Yuan, Jie He, Jing Jia, Meng-Yuan Yao, Sheng LianLuo, Chak-Tong Au, and Shuang-Feng Yin, Room temperature synthesis of Flower-like BiOX (X=Cl,Br,I) hierarchical structures and their visible light photocatalytic activity. Inorg. Chem., 2013; 52:111-118.
[5] Briand GG, Burford N. Bismuth Compounds and preparations with Biological or medicinal relevance. Chem Rev.,1999;99:2601-2658.
[6] Poznya SK, Kulak AI. Photoelectrochemical properties of bismuth oxyhalide films, Electrochim. Acta, 1990;35:1941-1947.
[7] K. Vasilev, J. Cook, H.J. Griesser. Antibacterial surfaces for biomedical devices. Expert Rev. Med. Devices 2009;6:553-567.
[8] H. Nagabhushana, R.B.Basavaraj, B. Daruka Prasad, S.C.Sharma, H.B. Premkumar, Udayabhanu, GR Vijaykumar. Facile EGCG assisted green synthesis of raspberry shaped CdO nanoparticles. Journal of Alloys and Compounds, 2016;669:232-239.
[9] Shiva kumara C, Saraf R. White luminescence of Dy3+ doped BiOCl phosphor and their Judd-Ofelt analysis. Dye. Pig., 2015;126:154-164.
[10] G.P. Darshan, H.B. Premkumar, H. Nagabhushana, S.C. Sharma, S.C. Prashanth, B. Daruka Prasad. Effective fingerprint recognition technique using doped yttrium aluminate nano phosphor material. Journal of Colloid and Interface Science. 2016;464:206-218.
[11] A.O. Ribeiro, P.S. Calefi, A.M. Pires and O.A. Serra, Characterization and spectroscopic studies of Eu3+ complexes with 3-phenyl-2,4-pentanedione, J. Alloys Comp.2004;374:151-153
[12] C.R. De Silva, J. Wang, M.D. Carducci, S. Asha Rajapakshe and Z.Zheng, Inner-salt structured lanthanide complexes as electroluminescent materials, Inorg. Chim. Acta, , 2004;357: 630
[13] S. Dutta, S. Som and S. K. Sharma, Excitation spectra and luminescence decay analysis of K+ compensated Dy3+ doped CaMoO4 phosphors. RSC Adv., 2015;5:73-80
[14] G. Blasse, Energy transfer in oxidic phosphors, Philips, Res. Rep.,1969;24:131-144
[15] L.G. Van Uitert, Characterization of Energy Transfer Interactions between Rare Earth Ions J. Electrochemical Society,1967;114:1048-1053.
[16] T. Manohar a, Ramachandra Naik, S.C. Prashantha , H. Nagabhushana, S.C. Sharma, H.P.Nagaswarupa K.S. Anantharaju, C. Pratapkumar, H.B. Premkumar, Photoluminescence and Judd-Ofelt analysis of Eu3+ doped LaAlO3 nanophosphors for WLEDs, Dye. Pig.,2015;122:22-30
[17] C.S. McCamy, "Correlated colour temperature as an explicit function of chromaticity coordinates, Color Res Appl., 1992;17:142-144.
[18] M. Saif, N. Alsayed, A. Mbarek, M. El-Kemary, M.S.A. Abdel-Mottaleb, Preparation and characterization of new photoluminescent nano-powder based on Eu3+:La2Ti2O7 and dispersed into silica matrix for latent fingerprint detection. Journal of Molecular Structure. 2016;1125:763-771.
[19] B. Errington, G. Lawson, S.W. Lewis, G.D. Smith, Micronised Egyptian blue pigment: a novel near-infrared luminescent fingerprint dusting powder, Dyes Pigments. 2016;132:310-315.